Published online 13 December 2007

Nucleic Acids Research, 2008, Vol. 36, No. 1 ***e2***
doi:10.1093/nar/gkm1094

siRNA nanoformulation against the Ret/PTC1 junction oncogene is efficient in an *in vivo* model of papillary thyroid carcinoma

Henri de Martimprey[1,2,*], Jean-Remi Bertrand[1], Alfredo Fusco[3], Massimo Santoro[3], Patrick Couvreur[2], Christine Vauthier[2] and Claude Malvy[1]

[1]CNRS, UMR 8121, Univ Paris-Sud, Institut Gustave Roussy, [2]CNRS, UMR 8612, Univ Paris-Sud, Faculté de Pharmacie and [3]Istituto di Endocrinologia ed Oncologia Sperimentale del CNR ''G.Salvatore'', c/o Dipartimento di Biologia e Patologia Cellulare e Molecolare, Universita' Federico II, Naples, Italy

Received July 27, 2007; Revised October 17, 2007; Accepted November 23, 2007

ABSTRACT

Delivery is a very important concern for therapeutic applications of siRNA. In this study, we have used chitosan-coated poly(isobutylcyanoacrylate) nanoparticles to deliver siRNA with a complementary sequence to the fusion oncogene ret/PTC1. By screening the mRNA junction we have selected a potent siRNA sequence able to inhibit this oncogene in a model of Papillary Thyroid Carcinoma cells. This siRNA sequence has then been validated by a shRNA approach using the same sequence. Furthermore, the high ret/PTC1 inhibition has triggered a phenotypic reversion of the transformed cells. We have designed well-defined chitosan decorated nanoparticles and succeeded to reduce their size. They have allowed to protect ret/PTC1 siRNA from *in vivo* degradation and leading to significant tumour growth inhibition after intratumoral administration.

INTRODUCTION

As with all nucleic acids, *in vivo* application of interfering strategy via siRNA or shRNA raises many challenges, such as transfection and tissue targeting (1,2). In fact, these molecules have excessive hydrophilic properties, and a poor *in vivo* stability. One pharmacological strategy is therefore to use vectors. Viral vectors are still the most powerful tool for gene transfection, because of their high efficiency in transduction, some of them being able to infect non-dividing cells. However, the death of J. Gelsinger in 1999, 4 days after an injection of adenovirus for a gene therapy trial (3) increased the attraction for the non-viral vectors approach. Non-viral vectors, although less efficient than viruses for gene delivery, offer however several advantages (4). They are particularly simple to use and can easily be produced at a large scale, and at a relatively low cost. It is easy to control their quality and they generate little or no specific immune responses. For these reasons, non-viral vectors have already become a powerful and popular research tool to elucidate gene structure, regulation and function. Various types of synthetic vectors such as cationic lipids and polymers have been developed for gene transfer and have proved efficient for the transfections. In these polyelectrolyte complexes, DNA is tightly packed, thus preventing the degradation by nucleases (5–7). These positively charged vectors are mainly cell internalized by non-specific electrostatic interactions (8). For example, chitosan, a positively charged polysaccharide containing non-acetylated beta-linked D-glucosamine residues has been intensively investigated as a nucleic acid delivery system. This polysaccharide extracted from chitine possesses a lot of qualities for DNA delivery such as the low cost of the vector, its easy to use and the biocompatibility. Since MacLaughlin's experiment (9), chitosan entered in the list of non-viral vectors. It has already been usefully utilized for the *in vivo* and *in vivo* delivery of siRNA as chitosan-based nanoparticles (10–13).

In the present study, we have used a new core-shell type of nanoparticles, where the core consisted of the biodegradable poly(isobutylcyanoacrylate) polymer and the shell of chitosan. These positively charged nanoparticles have never been used before as drug carriers for *in vivo* studies and the optimization of their synthesis allowed to dramatically reduce their diameter. The experimental treatment of papillary thyroid carcinoma by siRNA loaded onto those chitosan-coated poly(isobutylcyanoacrylate) nanoparticles was chosen here to exemplify the usefulness of this delivery approach.

Thyroid is the most frequently affected organ by endocrine cancers and represents 1% of all malignancies. Irradiation is the main traumatism responsible for thyroid

*To whom correspondence should be addressed. Tel: +33 142 115062; Fax: +33 142 115245; Email: martimprey@igr.fr

cancer development. Thus thousands of people developed thyroid cancers after the Chernobyl catastrophe (14,15). Thyroid cancers are observed in 57–87% of the malign tumours 5–8 years after the exposure and in 49–65% 7–11 years after (16). It is the eighth most common malignancy of woman cancer (17). Among all thyroid cancers, papillary thyroid carcinomas (PTCs), derived from follicular cells, are the most frequent, especially in radiation-associated thyroid carcinomas (18). It is due to a chromosomal rearrangement involving the *ret* receptor gene. *ret* encodes for a membrane tyrosine kinase receptor for a glial cell-derived neurotropic growth factor, and has a role in the regulation of growth, survival, differentiation and migration. ret is not normally expressed in thyroid follicular cells. Rearrangement involving the chromosome 10, between ret, and an ubiquitous gene leads to the abnormal expression of a chimeric constitutively activated ret protein in follicular cells. In the main cases it leads to the juxtaposition of the *ret* tyrosine kinase domain with *H4* gene (ret/PTC1 type) or with *ELE1* (ret/PTC3 type) (19,20). These rearrangements are consistently found in radiation-associated thyroid carcinomas (18) and are very frequent in clinically silent small thyroid tumours. Ret/PTC1 (the H4-ret fusion) is one of the most prevalent variants, especially in PTCs that occurred in children after the nuclear fallout in the Chernobyl area (14,21) and after external irradiation to medical treatment (18,22). The spatial proximity of ret gene with H4 during thyrocyte interphase can explain the ret/PTC1 formation (23). Despite a relatively low prevalence in adult PTCs, ret/PTC1 appears to be very dominant in pediatric PTCs (24).

The treatment of these cancers typically involves radioactive iodine, surgical resection, and lifelong levothyroxine medication. New technologies based on the inhibition of a specific gene involved in the development of thyroid tumour may be used to avoid or to lower the secondary effects of these treatments. They could also be used in the cases of resistance. Since ret/PTC1 plays a crucial role in the early stage of the tumour development (24), and is only present in the tumour cells, it appears to be a very good target for RNA interference based-treatment. This process consists in sequence-specific down-regulation by the use of short, double stranded RNAs named short interfering RNAs (siRNA). These siRNA are incorporated into a RNA-induced silencing complex (RISC) and serve as a template for sequence specific cleavage by RISC of the targeted mRNA. Cellular exonuclease activity induces complete degradation of the mRNA (25).

Such strategies have already been used for specific targeting and down-regulation of fusion oncogenes in chronic myeloid leukaemia and in a bone cancer, the Ewing sarcoma (26,27). In this study we extended this strategy to the human ret/PTC1 oncogene. For this purpose, we introduced the oncogene into NIH/3T3 murine fibroblast cells. These transformed cells were then used as a cellular model for *in vitro* and *in vivo* experiments. The importance of the ret/PTC1 gene in the cell transformed phenotype was then tested in order to establish if it constitutes a major target whose artificial blockage would result in an anticancer effect. In this view, we identified a sequence of siRNA, specific to the ret/PTC1 junction and able to silence the ret/PTC1 oncogene expression. Then ret/PTC1 silencing has been correlated with the phenotypic reversion to NIH/3T3 wild-type cells. This siRNA sequence can work as synthetic siRNA as well as a shRNA construction. As a first trial of the nanoparticles vector, we chose a intra-tumoral protocole. *In vivo* studies have confirmed the relevance of using chitosan-coated poly(isobutylcyanoacrylate) nanoparticles as a delivery system to inhibit the expression of ret/PTC1 as a treatment of the papillary thyroid carcinoma.

MATERIALS AND METHODS

Nucleic acids

The ret/PTC1 coding sequence cloned in a pBABE-puro plasmid containing the RET/PTC1 cDNA under the LTL promotor was kindly provided by Dr A. Fusco (University Federico II, Naples, Italy). Target sequences of siRNAs, named 1, 2, 3, 4 and 5, respectively, correspond to the human ret/H4 junction mRNA as indicated on the Figure 1. Specificity was tested using the BLAST search engine (www.ncbi.nlm.gov/BLAST), and excluding orthologous indentity, no siRNA had matches of more than 13 nucleotides to known human or murine mRNAs, or expressed sequence tags. RNAs were chemically synthesized and PAGE purified by Eurogentec (Belgium). 2′-Deoxynucleotides residues were used as the 3′ overhangs in the both sense and antisense strands so that it matched with mRNA sequences. Duplex formation was obtained by the preparation of 20 μM of sense and antisense RNAs aliquots in annealing buffer (Eurogentec) and then heating at 90°C for 1 min followed by a further incubation at 37°C for 1 h; aliquots were stored at −20°C.

An irrelevant sequence duplex siRNA was used as a control in the experiments. It was prepared from the RNA sequences given in Figure 1 according to the same procedure as described above.

Cell culture and transformation protocol

The NIH/3T3 cells were grown in DMEM medium (Gibco) containing 10% newborn calf serum inactivated by heat (Gibco) and a blend of antibiotics (100 U/ml penicillin, 100 μg/ml streptomycin, Gibco) at 37°C, 5% CO_2, in a moist atmosphere.

For plasmid transfection experiments, 10^6 cells were plated in a 100 mm dish. The plasmid was transfected into the cells with Superfect agent (Qiagen) as following. In a polystyrene tube, 1 μg of plasmid was diluted in 100 μl of 10 mM Hepes buffer pH 7.3, 100 mM NaCl. Then, 2 μl of Superfect (Qiagen) diluted in 100 μl of the same Hepes–NaCl buffer was added. After gently stirring, the mixture was incubated for 10 min at room temperature for complexes formation. Fresh medium was added to the cells and then, the 200 μl of DNA-Superfect dilution was then added to the cells in a fresh medium. After 48 h incubation, the medium was discarded and fresh medium containing selection agent was added for further time. Ret/PTC1 expressing cells where selected by adding 5 μg/ml puromycine (Sigma), and shRNA expressing cells

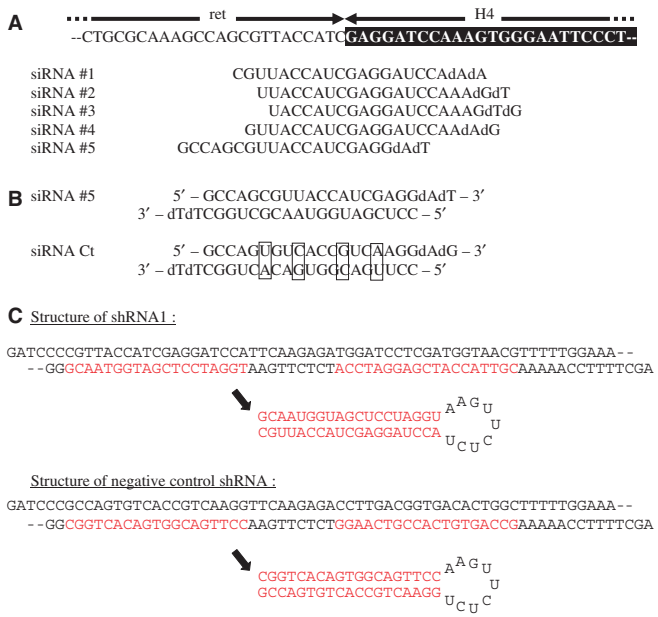

Figure 1. (**A**) Design of ret/PTC1 small interfering RNAs (siRNAs). Location of ret/PTC1 sense sequence of siRNA nos 1, 2, 3, 4 and 5 examined in this study are shown under the junction sequence of ret/PTC1. The H4 part of the oncogene is presented on the right part (■). (**B**) The control sequence is the sequence #5 with four mismatches. Mismatch site is shown in boxes. (**C**) Structure of the shRNA1 and negative control shRNA.

where selected by 1 mg/ml of Zeocine (Cayla) for 1 week and then 500 µg/ml for further time.

shRNA expression vector construction

We have cloned the sequence corresponding to the most efficient siRNA, the sequence designed as siRNA1, and the control sequence, designed as siRNA Ct, into the pTer plasmide (kindly provided by M. Kress, A Lwoff institute, Villejuif, France). The oligonucleotides contained a sense target sequence, a microRNA-based loop sequence of nine bases, and a antisense sequence, a termination sequence for polymerase III of five thymidines and appropriate ends for restriction enzymes in both ends. Thus, the resulting sequences for sequence shRNA1 and sequence shRNACt hairpins are:

5′-GATCCCCGTTACCATCGAGGATCCATTCAAGA GATGGATCCTCGATGGTAACGTTTTTGGAAA-3′ as sequence shRNA1 sense
5′-AGCTTTTCCAAAAACGTTACCATCGAGGATCC ATCTCTTGAATGGATCCTCGATGGTAACGGG-3′ as sequence shRNA1 antisense
5′-GATCCCGCCAGTGTCACCGTCAAGGTTCAAG AGACCTTGACGGTGACACTGGCTTTTTGGAAA-3′ as sequence negative control shRNA sense
5′-AGCTTTTCCAAAAAGCCAGTGTCACCGTCAAG GTCTCTTGAACCTTGACGGTGACACTGGCGG-3′ as sequence negative control shRNA antisense (see Figure 1C).

Duplexes where formed by heating 5 min at 95°C the complementary sequence in annealing buffer (50 mM Tris, pH 7.5, 100 mM NaCl in MilliQ water). The mixture was cooled at 70°C for 10 min before allowing it to return at room temperature. The duplexes were then phosphorylated by T4 Poly Nucleotide Kinase (New England Biolabs) using the shipper protocol. After linearization of the pTer plasmid by BglII and HindIII restriction enzymes, the shRNA sequence was cloned, giving two plasmids pTer-shCt and pTer-sh1.

siRNA treatment

The effect of siRNAs was measured after cell transfection with Cytofectin GSV (GTS). Pratically, 2×10^5 cells/well were seeded in 35 mm tissues culture dishes. Then, three successive transfections were done at the time 8 h, 24 h and 48 h. The transfection solution was prepared as following: 0.05 nmol of siRNA were diluted in 50 µl of a solution containing 100 mM NaCl, 10 mM Hepes buffer pH 7.3. A volume corresponding to 2 µg of Cytofectine (GSV) was then diluted in 50 µl of 100 mM NaCl, 10 mM Hepes buffer pH 7.3 and then added to the siRNA solution. The complexes formation was obtained after 10 min incubation at room temperature and gently mixing. The complexes were then dropped on the cells in a fresh culture medium containing serum.

Detection of RET/PTC1 mRNA expression by RT-PCR

The mRNA extraction was performed with the TRIzol reagent (Invitrogen) as indicated by the shipper from the cells of each well. After concentration determination and good quality control, 1 µg of total RNA from treated or control cells were incubated in 20 µl final volume of M-MuLV RT (promega, France) for 1 h at 42°C. Then ret/PTC1 mRNA expression was determined by PCR on 2 µl of the reverse transcription product in 50 µl final volume with Taq polymerase (Biolabs). The following primers were used for ret/PTC1 amplification (290 bp): forward 5′-AGATAGAGCTGGAGACCTAC-3′ and reverse 5′ CTGCTTCAGGACGTTGAA 3′; for GAPDH (531 bp): 5′ GACAACTCACTCAAGATTGT CAG 3′ and 5′ CATTGTCATACCAGGAAATG 3′. The PCR product of ret/PTC1 and GAPDH were observed at 290 bp after 35 cycles and 531 bp after 32 cycles, respectively. PCR products were analysed on a 2% agarose gel TAE [0.5×] under 8.3 V/cm The fragment was observed under UV after staining with ethidium bromide 0.5 µg/ml. A 100 bp ladder (New England Biolabs) was used as a standard.

Real-time quantitative PCR

Cells were lysed using TRIzol reagent (Invitrogen, France) and total RNA was recovered according to the manufacturer instructions.

The tumour extraction was performed as following. The subcutaneous tumours were sampled and immediately freeze in liquid nitrogen. The tumour were then crushed in TRIzol reagent (Invitrogen, France) in a FastPrep 24 (MP Biomedicals) and the RNA was recovered according to the manufacturer instruction. The RNA was then incubated in a DNase, RNase free medium for 1 h.

Total RNA was quantified using the ND-1000 spectrophotometer (Nanodrop). Superscript II Reverse Transcriptase kit (Invitrogen) was used for reverse transcription. The same primers as for RT-PCR were used for the amplification of ret/PTC1. Taq Universal PCR Master Mix (Applera) was used as fluorescent dye. Samples were amplified for 50 PCR cycles with continuous monitoring of fluorescence. 18S gene was used as a PCR control using Human 18S rRNA MGB kit (Applera). The Ct of the genes are respectively between 12 and 16 for 18S, and between 20 and 27 for ret/PTC1. The amplification was monitored on an ABI prism 7700 real-time PCR apparatus (Perkin–Elmer).

Protein studies

Immunoblotting experiments were performed according to standard procedures. Briefly, cells were harvested in lysis buffer (RIPA solution) containing Tris 50 mM, NaCl 150 mM, EDTA 1 mM glycerol 10%, NP 40 0.5% and complete protease inhibitor (Roche, Germany). Protein concentration was determined using BCA protein assay (Pierce). After transfer on BAF-83 nitro cellulose (Schleicher & Schuell) protein were detected with specific antigens. Detection was performed by chemiluminescence kit (ECL, Amersham). Anti-ret (C-term) antibodies were from Abgent, and anti-actin were from Santa Cruz Biotechnology.

Cytochemistry of stress fibre

The cells were plated at a concentration of 1.5×10^5 cells/well in 6-well plates containing a cover glass. After 3 days of treatment as previously described, the medium was removed and the cells were washed with PBS, and then fixed with formaldehyde 4% in PBS for 20 min at 4°C. The formaldehyde was then neutralized by a solution of 50 mM NH_4Cl in PBS before treatment with 0.4% Triton X100 in PBS. RNA were discarded by 30 min treatment with 10 μg/ml RNase A in PBS at room temperature. The cover glass was then stained with 600 nM DAPI and 40 U/ml of FITC-conjugated phalloidin in PBS buffer. The slides were observed with a microscope Nikon eclipse E600 equipped with CCD camera.

Synthesis of nanoparticles by redox radical emulsion *polymerization*

Chitosan was hydrolysed as indicated by Bertholon *et al.* (28), to reach a final molecular weight of 20 kDa. Chitosan (0.137 g) was dissolved in 8 ml of 0.2 M nitric acid aqueous solution. After 10 min at 40°C under argon bubbling, 0.3 g of Lutrol F68 (BASF) was dissolved in the solution, followed by the addition of 2 ml of 80 mM $Ce(NH_3)_2(NO_3)_4$ in 0.2 M HNO_3 and 0.5 ml of isobutylcyanoacrylate (kindly provided by Henkel Biomedical) under vigorous stirring. Polymerization was performed under vigorous stirring for 50 min. Gentle argon bubbling was maintained during the first 10 min. Then, the reaction medium was cooled at 15°C and pH was increased until 6.0. Nanoparticles were purified by dialysis against MilliQ water (MWCO: 100 000; 2×1 l, 2 h and 1 l overnight), providing a slightly turbid solution.

Nanoparticles characterization

Particle size. The hydrodynamic diameter of the nanoparticles was measured at 20°C by quasi-elastic light scattering using a Nanosizer N4 PLUS (Beckman-Coulter, France), operating at 90°. Sixty microlitres of each sample was diluted in 2 ml of MilliQ water. The temperature was allowed to equilibrate 5 min before measurement. The results gave the mean hydrodynamic diameter of the dispersed particles obtained from three independent determinations. The standard deviation of the size distribution and the polydispersity index were also given.

Zeta potential. A good estimation of the surface charge of the particles is the measure of their zeta potential. It was measured using a Zetasizer 4 (Malvern Instrument Ltd, France). Dilution of the suspensions [1:33 (v/v)] was performed in NaCl 1 mM.

Transmission electron microscopy. Transmission electron microscopy (TEM) was performed using a Philips EM208 with a large format CCD camera AMT at the CCME Orsay. The samples were diluted in MilliQ water 1:100 and deposited on a carbon-coated formwar film on copper grids. After 5 min, the excess was removed and stained with neutral 1% aqueous phosphotungstic acid during 30 s.

Preparation of ^{32}P-labelled siRNA

SiRNA #1 were labelled at the 5′-end by T4 polynucleotide kinase (New England Biolabs) and [γ-^{32}P]ATP (Amersham Bioscience) in 50 μl of reaction mixture. Thus, 5 μl of siRNA #1 stock solution (20 μM), RNase-free water (30 μl), 10× kinase buffer (5 μl; New England Biolabs), 5 μl of T4 polynucleotide kinase (10 U/μl), and 5 μl of [γ-^{32}P]ATP (>5000 Ci/mmol) were incubated at 37°C for 1 h, and 20 min at 65°C. The reaction mixture was placed in the upper chamber of MicroCon YM3 (cutoff value M_r 3000; Millipore). After adding 200 μl of RNase-free water, it was centrifuged (4000*g*). The procedure was repeated four times. Material remaining in the upper chamber was regarded as γ-^{32}P-labelled siRNA #1.

siRNA adsorption on nanoparticles

Nanoparticle (NP) suspensions were diluted in MilliQ water at different concentrations to reach the following mass ratios nanoparticles/siRNA (0; 10; 20; 25; 30; 40; 45; 50; 100 and 300). The ^{32}P-labelled siRNA was added to each nanoparticle suspension to reach a final siRNA concentration of 0.5 μM in a final volume of 300 μl. Liquid paraffin was then added to equilibrate the tubes for ultracentrifugation. After 10 min of incubation, the suspension was ultracentrifuged in a 70.1 Ti rotor at 45 000 rpm (average g-force: 138 915) at 4°C for 1 h. The radioactivity of 100 μl of supernatant was measured for non-adsorbed siRNA quantification.

PAGE anlaysis of γ-^{32}P-labelled siRNA injected into the tumour

γ-^{32}P-labelled siRNA associated with nanoparticles was injected into RP1 tumours. After 24 h and 48 h of

injection, each tumour was excised and homogenized in 0.5 ml of ice cold Tris–HCl (pH 8.0) with 0.1% Triton X-100, 50 mM NaCl, and RNase inhibitor (1 U/μl, Roche) and then centrifuged. Proteinase K (1 mg; Roche) was directly added to the supernatant and incubated for 6 h at 37°C and centrifuged (1000*g*; 10 min). The supernatant was analysed by PAGE (10% gel) followed by autoradiography.

Animal experiment

All animal experiments were carried out according to the French Laws of animal welfare and were approved by the Ethics Commission of the official veterinary authorities.

The tumorigenicity tests were performed on nude mice product by the laboratory. The mice were pre-irradiated by 5 Gy 1 day before tumour implant. 10^6 living cells were injected subcutaneously into the right flank of nude mice. The tumour sizes determination was performed with by a digital slide caliper, and the tumour volume in cubic millimetres was calculated by the formula: volume = $(\text{width})^2 \times \text{length}/2$. Data are presented as mean ± SE.

After 1 week, when the tumours reached a volume of ~50 mm^3, the tumour bearing nude mice were treated with siRNA #1 and siRNA Ct. Four micrograms of siRNA complexed with, or without, 200 μg of nanoparticles were diluted in 100 μl 0.9% saline before injection. As positive control, physiological serum or nanoparticles diluted in physiological serum were injected. Each therapeutic reagent was injected into the tumour every 2 days after the first injection, as indicated in Figure 6B. A final volume of 100 μl was intratumoral injected.

RESULTS

Nanoparticles characterization

As shown by Bertholon *et al.* (28) the size of the final nanoparticles is tightly related to the molecular weight of the chitosan used during the polymerisation process. Hydrolysis of the commercial chitosan up to a 20 kDa molecular weight decreased the size of the nanoparticles to 178 nm. The use of a surfactant allowed to dramatically decrease the size of the obtained nanoparticles. Indeed, the addition of Lutrol F68 reduced the hydrodynamic diameter of the nanoparticles from 107 nm with 1% (*m*/*v*) to 41 nm with 4% (*m*/*v*) (Figure 2A). These results were consistent with the observed reduction of the solution turbidity. No reduction was obtained by addition of the lutrol 68 after the polymerisation. The size reduction is due to a nanoparticle core size reduction, not to a collapse of the chitosan brush (data not shown). Until now, it was only possible to prepare nanoparticles with size over 200 nm (29), thus reducing size is new. This is an important fact as too big nanoparticles cannot enter cells efficiently and too small particles cannot remain and accumulate in the tumours after translocation through the wide fenestration of the tumour endothelium (the so-called 'Enhanced Permeability and Retention Effect') (29). We have thus chosen to use medium sized nanoparticles of 60 nm (i.e. 3% Lutrol F68) for the *in vivo* study, that can penetrate cells and accumulate.

As shown in Figure 2B, these nanoparticles appeared round-shaped at TEM with a size of ~30 nm and they did not aggregate. Since drying of the sample was needed before TEM observation, the chitosan brush, naturally expanded in water, was completely folded up on the polymeric surface. This explains the observed lower size at TEM (30 nm) comparatively to the 60 nm measured by quasi-elastic light scattering, since the hydrodynamic diameter take into account the thickness of the chitosan brush too.

These nanoparticles displayed a positive value of the zeta potential (+26 mV) due to the chitosan surface (Figure 2E, ratio siRNA/nanoparticles = 0) which insured an excellent colloidal stability to the suspension. No change in the zeta potential nor in the size of nanoparticles was observed after 10 months conservation at 4°C. A light white deposit was observed that could be resuspended by gentle agitation.

Adsorption of the siRNA on the nanoparticle surface

When mixing positively charged chitosan-decorated nanoparticles with negatively charged siRNA, nanoplexes could be obtained (Figure 2C). For a ratio nanoparticles/si RNA of 50, siRNA adsorption onto nanoparticles reached ~90% (Figure 2D). Noteworthy, no modification of the adsorption isotherm was observed when a 10-month old nanoparticle preparation was used, confirming the high stability of the nanoparticles suspension.

The adsorption of siRNA onto the nanoparticles surface was further investigated by measuring the zeta potential of the particles according to the addition of increasing amount of siRNA (Figure 2E). As expected, siRNA adsorption induced a negative zeta potential value of the nanoplex, and the more siRNA was added, the more the zeta potential was negative. The mass ratio 1/50 (siRNA/nanoparticles) led to a resulting zeta potential of −11.8 mV. No significant modification of the nanoparticle size was observed after siRNA complexation.

Tumoral transformation of the cells

NIH/3T3 cells were stably transfected by the ret/PTC1 expression plasmid, giving the RP1 cell line. The ret/PTC1 mRNA expression was determined on the RP1 cell line and was associated to some morphological modifications (Figure 3).

NIH/3T3 murine fibroblasts were characterized by a monolayer growing with a flat aspect and generally possessing four angular extremities. The introduction of the ret/PTC1 oncogene into NIH/3T3 cells changed their morphology with a difringent round aspect with two extremities (Figure 3A).

The shape modification is a marker of deep cytoskeleton reorganization. The NIH/3T3 fibroblasts have a flat aspect associated to a well-organized actin fibre. The round refringent aspect of the RP1 cell line is associated to a loss of these actin fibres with an homogenous green colored cytoplasm (Figure 3B).

We observed that the parent NIH/3T3 cells grew as a mono-layer and stopped dividing when confluence occurred. In the case of RP1 cells, they go one over the

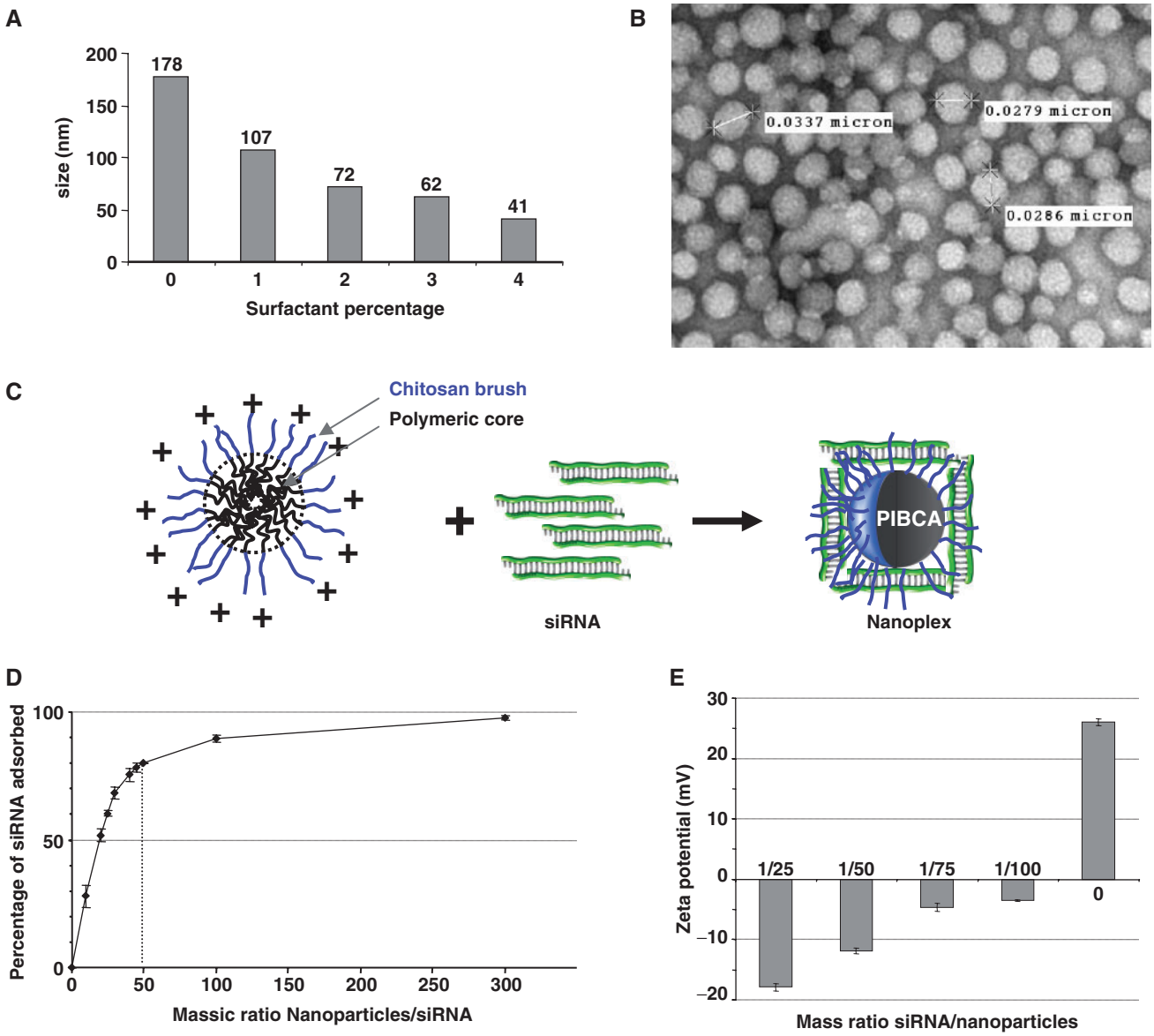

Figure 2. (**A**) Influence of the addition of Lutrol F68 in the polymerization medium. (**B**) TEM image of the nanoparticles after 1% aqueous phosphotungstic acid staining. (**C**) Schematic representation of siRNA adsorption onto nanoparticle surface. PIBCA: the poly(isobutylcyanoacrylate). (**D**) Adsorption isotherm of ret/PTC1 siRNA at the surface of nanoparticles. (**E**) Zeta potential of the nanoparticles according to the amount of siRNA adsorbed.

other to form cell aggregates showing a loss of cell-contact inhibition. This ability to grow without support attachment resulted in big floating aggregates. This is typical of a tumorigenic transformation of the cells. As it is shown on the Figure 3C, the RP1 cells formed aggregates even without monolayer of cells. This result pleads in favour of a cell chemioattraction. Moreover growth continued after confluence as observed by the MTT test (data not shown).

Screening of the ret/PTC1 siRNA sequences in cells

As presented in Figure 4B, we compared the different siRNAs of Figure 1, targeted on the oncogene junction area. Using similar experimental conditions for all siRNAs, the number one was found to be the most efficient after RT-PCR quantification of ret/PTC1 expression inhibition. Thus, siRNA #1 was chosen for further experiments. Control siRNA showed no effects. The Q-PCR analysis revealed an 89% ret/PTC1 mRNA inhibition for treated cells compared to untreated RPI cells (Figure 4C). Western blot analysis confirmed the down-regulation of the ret/PTC1 oncoprotein by transfection of the siRNA. It can be seen in Figure 4D that the two bands of 64 kDa and 59 kDa corresponding to the two isoforms of the ret/PTC1 oncoprotein were down-regulated. We also investigated the reorganization of the actin stress fibres as a phenotypical reversion associated with the down-regulation of ret/PTC1. RP1 cells receiving control siRNA still lack stress fibres in the cytoplasm.

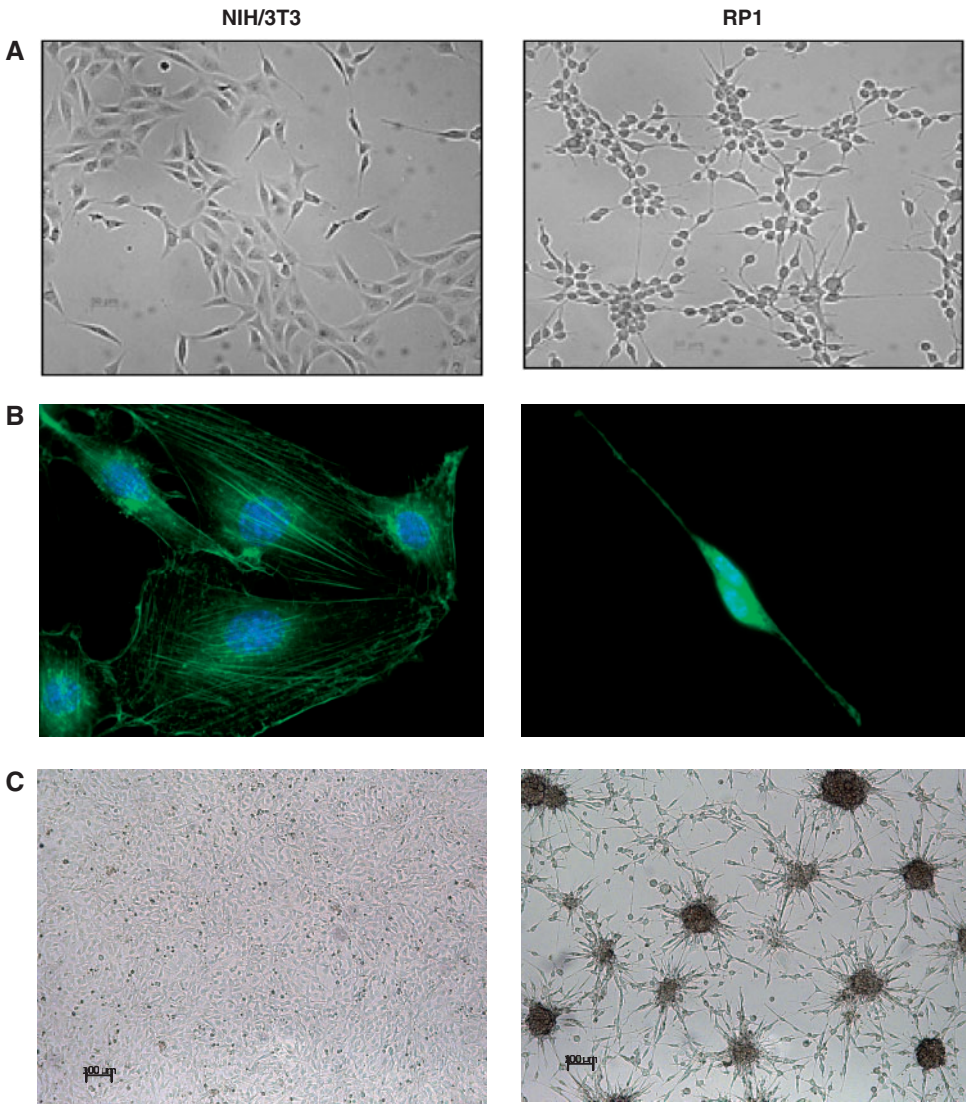

Figure 3. Phenotypicals features of the NIH/3T3 cells and of the ret/PTC1 transformed NIH/3T3 cells, named RP1. (**A**) Not confluent cells (phase contrast). (**B**) Cytochemistry coloration of actin fibres (falloidine-FITC and DAPI coloration). (**C**) Confluent cells (phase contrast).

After siRNA treatment, stress fibres of actin appear in the cytoplasm, confirming the reorganization of actin in fibres, as observed in NIH/3T3 mother cells (Figure 4E). Transfection of RP1 cells with the fluorescent siRNA #1 gave a characteristic spotty distribution of fluorescence around the nuclei (Figure 4A).This is consistent with an uptake of the siRNAs after transfection.

In vitro effect of the shRNA expression plasmid

To overcome the poor *in vivo* stability of siRNA, we then shifted to the shRNA strategy containing a H1 promotor. RP1 Cells were transfected and selected in medium containing zeocin. After selection, individual colonies were isolated and the knockdown of the ret/PTC1 oncogene was tested by RT-PCR. Two clones of pTer-sh1 transformed cells were selected with two different levels of ret/PTC1 inhibition. The cells expressing the control shRNA gave no difference compared to mother cells RP1. Aggregates could still be observed, and the cells remained to have a round shape. On the contrary, cells expressing the antisense shRNA, returned to have contact inhibition, no aggregates were visible, and the cells had a flattened form. Q-PCR evaluation confirmed the ability of pTer-sh1 to inhibit the ret/PTC1 oncogene. Two clones resisting to zeocin, (sh1-11 and sh1-19) were selected with two different levels of ret/PTC1. sh1-11 and sh1-19 have a residual ret/PTC1 expression of, respectively 4% and 36%, in comparison with RP1 mother cells (Figure 5A). The expression vector of the shRNA control, pTer-shCt, was unable to down-regulate the ret/PTC1 oncogene in RP1 cells. One clone resisting to zeocin, shCt was selected as control clone. Q-PCR revealed an expression rate of ret/PTC1 of 93% (Figure 5A). These results were confirmed by western blot analysis on the three clones (Figure 5B). Finally inhibition of ret/PTC1 in RP1 cells by pTer-sh1 plasmid induced actin fibre reorganization whereas no actin fibres were observed with the pTer-shCt.

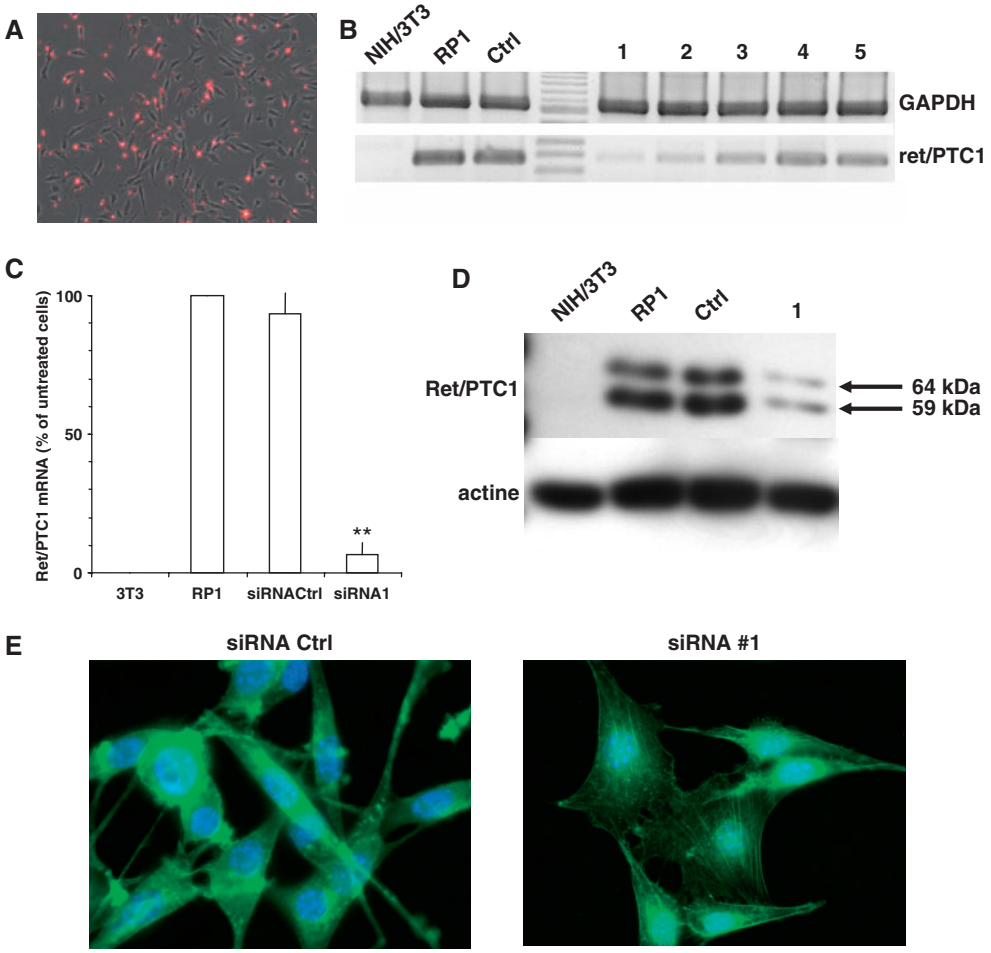

Figure 4. Analysis of the inhibition of ret/PTC1 by cytofectine transfected siRNA *in vitro*. (**A**) Penetration of the Rhodamine-labelled siRNA into RP1 with cytofectine. (**B**) Effect of siRNA target sequence on ret/PTC1 expression by RT-PCR. The siRNA were transfected by cytofectin GSV with a final concentration of 50 nM. (**C**) Q-PCR and (**D**) western blot analysis of the most efficient siRNA #1 transfected by cytofectin. (**E**) Cytochemistry of stress fibres in RPI cells transfected with control siRNA (Ctrl) or antisense siRNA #1. Three siRNA transfections were performed before analysis. $^{**}P < 0.001$ versus RP1.

It was interesting to observe that low inhibition of the ret/PTC1 was not able to reverse the phenotype as for sh1-19 whereas an important inhibition of the oncogene, as observed in sh1-11, was able to completely reverse phenotypic inhibition (Figure 5C).

In vivo tumorigenic effect of shRNA pretreated RP1 cells

After subcutaneous injection of 10^6 living cells from each clone into the flank of irradiated nude mice, tumours became visible on the RP1 injected group ($n = 30$). The tumoral growth was then followed during 17 days. The results are given on Figure 6A where it can be seen that after 17 days, the RP1 cells and the shCt reached a volume of 4000 cm^3, whereas the sh1-19 cells reached only 263 cm^3 and no tumour growth was visible for the NIH/3T3 and the sh1-11 treated animals. Post-mortem analysis revealed no tumour nodule peripheral organ. A light increase in the volume of the spleen was just observed. The tumoral growth was then related to the expression of ret/PTC1 in NIH/3T3 cells. No loss of body weight was observed during the experimental period (data not shown).

In vivo treatment of a RP1 derived tumour by ret/PTC1 siRNA

Fifteen days after subcutaneous injection of RP1 cells (1.0×10^6) into the flank of irradiated nude mice, tumour nodules were observed (mean tumour volume: 43.35 mm^3; $n = 30$). For the determination of the therapeutic effect of ret/PTC1 siRNA, intratumoral injections of siRNA loaded onto nanoparticles or nanoparticles alone were started and repeated for a total dose of siRNA of 1 mg/kg in five injections. As a first trial with the new siRNA, we have chosen to perform intra-tumoral injections instead of systemic injections. In fact, by using systemic injection, the uncertainty about the bio-distribution of a new formulation can be an additional obstacle compromising the initial *in vivo* evaluation of the drug cellular efficiency. The tumour delivery efficiency of the new formulation is one of our goals. This choice was also based from our previous experience on the Ewing Sarcoma (27).

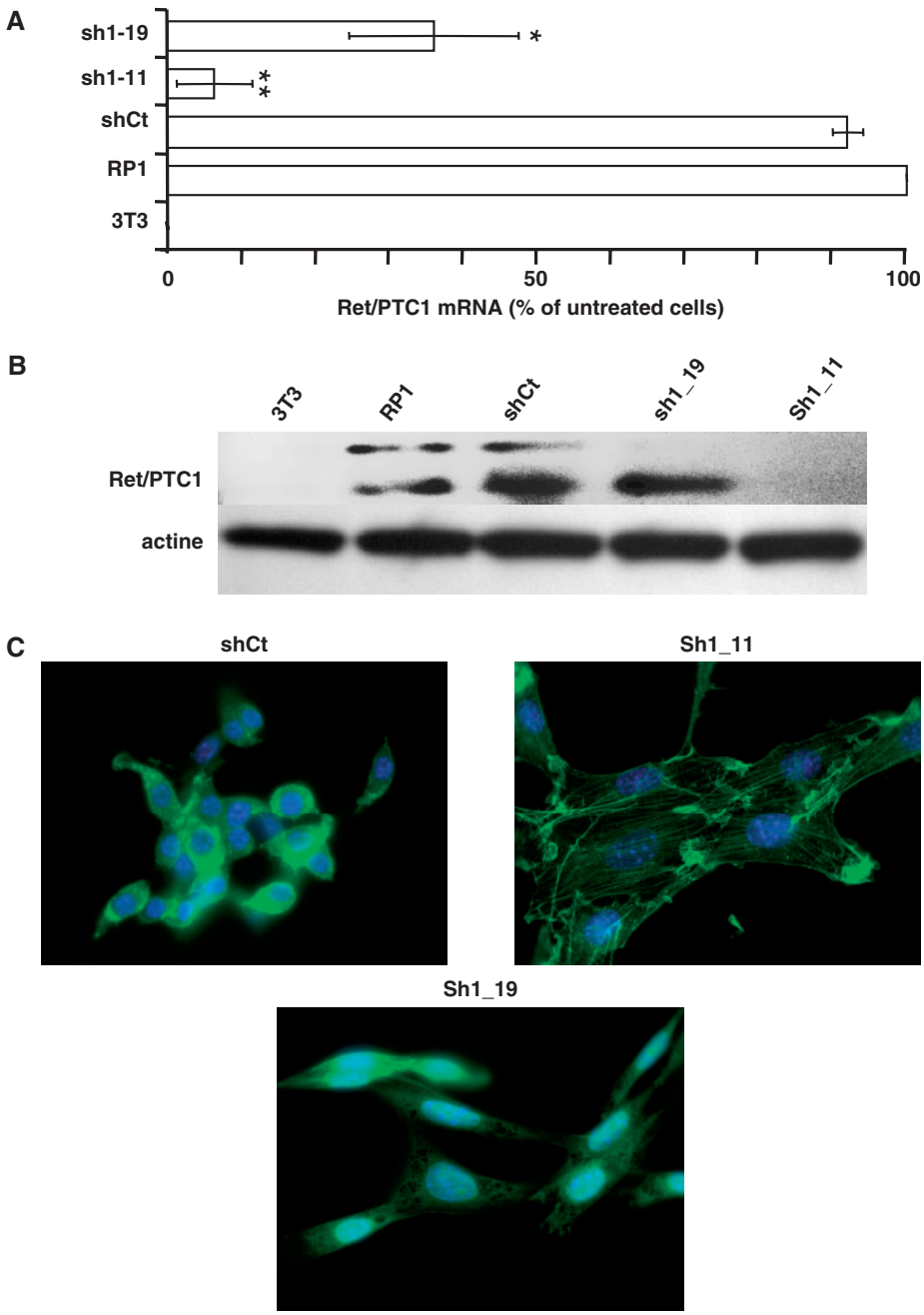

Figure 5. *In vitro* shRNA inhibition of ret/PTC1. (A) and (B) Q-PCR and western blot analysis of the clones expressing the shRNA. ShCt expresses the negative control sequence, sh1_11 and sh1_19 express the specific shRNA at various levels. (C) Cytochemistry of stress fibres in clones expressing the shRNA. $^{*}P < 0.05$ and $^{**}P < 0.001$ versus RP1.

As shown in Figure 6B, only ret/PTC1 siRNA1 complexed with the nanoparticles significantly inhibited tumour growth as compared to ret/PTC1 siRNA free, to siRNA control (complexed or not with nanospheres) or to nanoparticles alone ($P < 0.05$). Q-PCR analysis of the tumoral mRNA reveals a high down-regulation of the expression of ret/PTC1 gene after siRNA #1/nanoparticle treatment. No significant inhibition of the gene was observed after control siRNA treatment associated with nanoparticles or by free nanoparticles (Figure 6C).

5′-Radiolabelling of the siRNA by a Poly Nucleotid kinase allowed us to detect its intact form 48 h post injection. At this time a significant amount of radiolabelled siRNA remains intact in the tumour after nanoparticules association whereas the intact form is no more observable without nanoparticles complexation (Figure 6D).

Statistical analysis

GraphPad Instat software was used for the statistical analysis. The ANOVA test was performed.

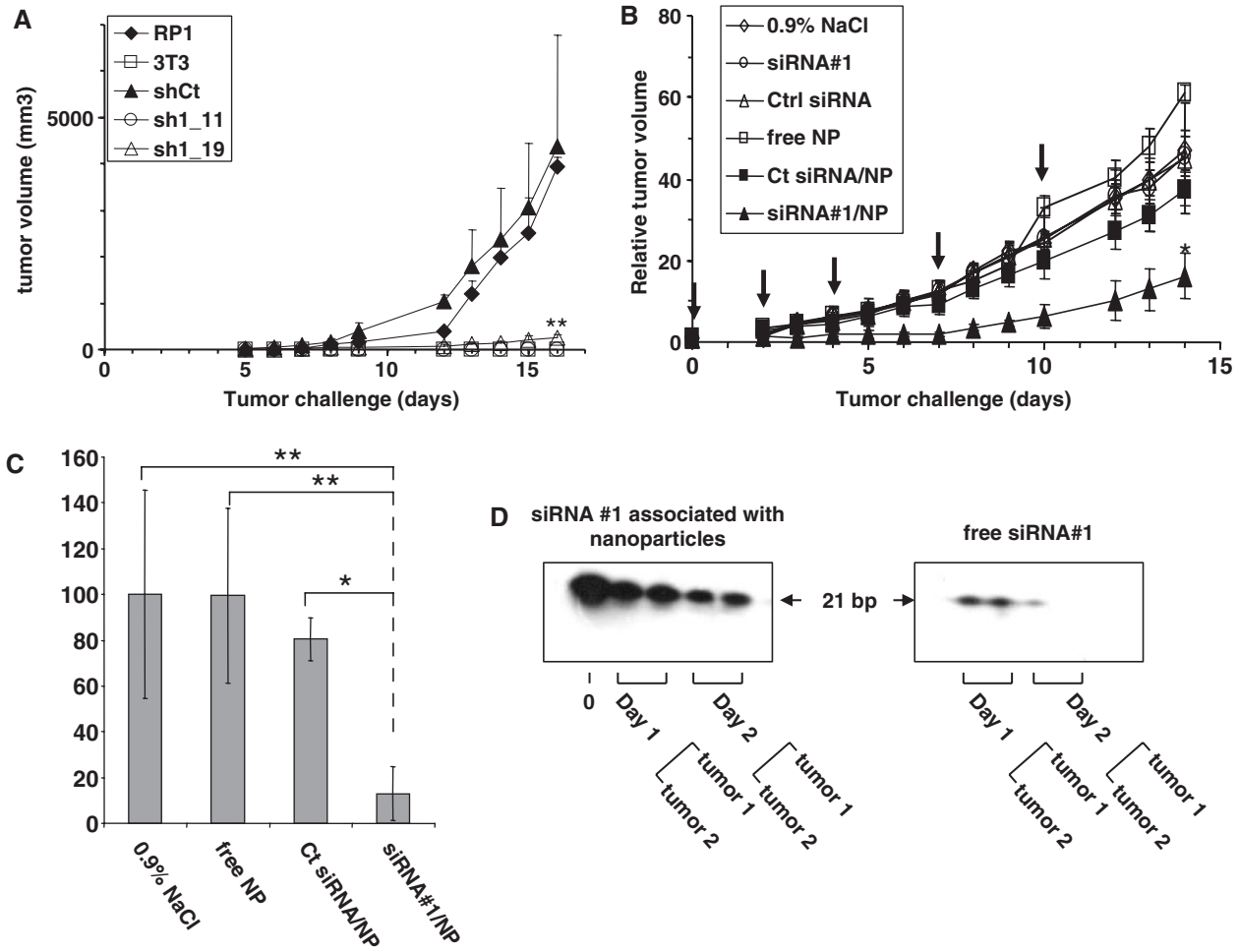

Figure 6. *In vivo* studies. (**A**) Tumoral growth of the different shRNA clones after grafting on the right flanc. $^{**}P < 0.001$ versus RP1. (**B**) Antitumor effect of the ret/PTC1 small interfering RNA (siRNA) in the RP1 graft. Injections were performed on days 0, 2, 4, 7, 10 as indicated by the arrows. siRNA were dissolved in 0.9% NaCl. The following preparations were intratumorally injected: free siRNA #1 (siRNA #1), free control siRNA (Ctrl siRNA), unloaded nanoparticles (free NP), siRNA #1 associated with nanoparticles (siRNA #1/NP) and control siRNA associated with nanoparticles (Ctrl siRNA/NP). $^{*}P < 0.05$ versus 0.9% NaCl-treated mice. (**C**) Q-PCR analysis of the ret/PTC1 expression in tumor tissues at day 11 after the first injection. (**D**) stability of nanoparticles-associated ^{32}P-labelled siRNA and free ^{32}P-labelled siRNA after intratumoral injection. The total RNA was extracted from tumor and analysed by PAGE as described in materials and methods. Experiments start at the first injection.

DISCUSSION

Many researchers consider siRNAs as promising therapeutic agents. However, RNA is a fragile molecule which is degraded in biological fluids and poorly diffuses through the cell membrane. This is the reason why non viral vectors are needed to allow their efficient delivery *in vivo*. However, in view of their possible use in clinic, artificial carriers require to be biocompatible and well characterized. This is the reason why we propose, in the present article, to use chitosan-coated biodegradable poly(isobutylcyanoacrylate) nanoparticles for the administration of a siRNA oriented towards the junction oncogene in the papillary thyroid carcinoma. This carcinoma is mainly due to a paracentric inversion of the chromosome 10. This leads to the fusion of the 5′ sequence of ret with the 3′ part of an ubiquitously expressed gene, H4. As a result, the gene under the H4 promotor, is abnormally expressed in follicular cells and the chimerical protein is re-localized in the cytoplasm compartment and constitutively activated (20). To develop a new strategy based on gene inhibition it was important to control whether the modulation of ret/PTC1 expression was or was not associated with the tumorigenicity of thyroid carcinoma cells. For this purpose, we used a model of tumour cell obtained by the introduction of this human oncogene into murine fibroblasts NIH/3T3. We observed that the expression of the *ret*/PTC1 gene was sufficient to transform the NIH/3T3 cells from immortal and not tumoral to tumoral. Noteworthy non transformed NIH/3T3 cells were unable to form tumor after grafting in nude mice, confirming the absence of transformation of the commercial cell line. The ret/PTC1 transformed NIH/3T3 cell line reversibly became spindle-shaped or round as was already observed by others (30). Such shape transformation is the consequence of cytoskeleton reorganization. Indeed, it is

known that NIH/3T3 cells have well-developed actin stress fibres (31). We have confirmed these data, but in addition, we have shown that expression of ret/PTC1 in these cells induced a complete disorganization of actin fibres (Figure 3B). This effect seemed to be related to cells that have naturally stress fibres, such as NIH/3T3 transformed cells. In fact, ret/PTC1 expression induced actin organization in stress fibres in PC Cl 3 rat thyroid cells, that naturally lack actin stress fibres (32). Barone *et al.* explained this result by the fact that ret/PTC1 signalization pathways differ in thyroid cells and fibroblasts. In fact, the chimerical protein ret/PTC1 activates BRAF through Grb2/SOS>RAS pathway and Grb2/Gab1 > Rap1 pathway (33). In PC Cl 3 cells, Rho activation through Rap1 induces actin stress fibres formation (32,34). On the contrary, in the NIH/3T3 model used here, the Phosphoinositide 3-OH Kinase and Ras, both activated by ret/PTC1 (20,35), induced actin stress fibres disorganization and morphological changes *via* ERK (31). The NIH/3T3 cell model is nevertheless an interesting model to test the efficiency of artificial ret/PTC1 down-regulation because of its strict ret/PTC1 phenotype dependency. For a pharmacological approach, we have made the choice of the siRNAs as potential therapeutic molecules. Before undertaking expensive *in vivo* experiments it was necessary to check the validity of ret/PTC1 as a relevant antitumor target. The shRNA strategy offers the advantage of long term inhibition of the studied gene and greatly facilitates the *in vivo* estimation of the target validity. Using the siRNA sequence selected as the most efficient one to inhibit ret/PTC1 we have integrated it in a plasmid construction and shown that the selected cells displayed a permanent inhibition of ret/PTC1 (96% inhibition for the shRNA in sh1-11 clone). We found that inhibition of the ret/PTC1 oncogene by shRNA was able to completely reverse the RP1 phenotype in culture. In order to obtain a better relationship between oncogene inhibition and phenotype reversion, we selected two clones with different level of ret/PTC1 down-regulation. The oncogene inhibition by the shRNA in sh1-19 clone provided a lower inhibition than in sh1-11 clone with 36% of ret/PTC1 expression left instead of 4%. The different levels of inhibition by the shRNA into the cells can be explained by the clone selection. Selected clones have, indeed, chromosomal integration of the transfected plasmid. As a result, the shRNA concentration in the cytoplasm will depend on integration regions and will be variable. Accordingly, we have found that the inhibition of ret/PTC1 by shRNA was dependent on the selected clone. The protein analysis by western blot has confirmed these results. Further *in vivo* studies have demonstrated ret/PTC1 oncogene silencing. No silencing or low silencing (less than 64% silencing) induced tumor growth but 90% silencing resulted in tumoral growth inhibition. As a conclusion, antitumoral effect by silencing the oncogene needs a very high level of inhibition.

Although powerful, the shRNA strategy requires the selection of clones which might not be representative of the whole cell population. Therefore, it was necessary to directly evaluate the effect of siRNAs on the RP1 phenotype, This could be obtained after 3 transfections, without any sign of cytotoxicity regarding MTT assays (data not shown); additionally, no actin stress fibres modification was observed after transfection of the control siRNA using cytofectine. By applying the same transfection protocol for the siRNAs, 89% inhibition of ret/PTC1 could be obtained *in vitro* for several days. Despite such high ret/PTC1 inhibition, measured by PCR and western blot, the actin skeleton of individual cells did not appear to be homogeneous. Only a significant population of cells had complete phenotypic reversion whereas few cells did not have complete actin stress fibres reorganization. These data highlight the problem of the individual cell transfection heterogeneity. Nevertheless, the phenotypic reversion was very similar to that obtained with the shRNA. The validity of ret/PTC1 as an antitumor target was therefore, demonstrated. It was also demonstrated that this characteristic of ret/PTC1 expression was not related to the selection of a few clones. Further experiments were also needed to check for an always possible additive off-target effect of our RET/PTC1 siRNA in the phenotypic reversion of RP1 cells. However, the NIH/3T3-NIH/3T3 RP1 system where RP1 differed initially from NIH/3T3 only by the RET/PTC1 protein expression argues for a non necessary additional gene inhibition to the RET/PTC1 inhibition in the phenotypic reversion. According to our initial hypothesis targeting junction oncogenes, rather than oncogenes, with punctual mutations or modifications of their expression regulation should result in a better specificity of the siRNA. In fact, the lack of specificity is the main cause of side effects in preclinical trials (36). Taking into account the results described above, off target effects and specificity of siRNA targeting junction oncogenes could be evaluated *in vivo* using nanoparticles.

For performing the *in vivo* experiments with RET/PTC1 siRNA, we have employed, for the reasons explained before, the previously described chitosan/poly(isobutylcyanoacrylate)core-shell nanoparticles prepared by radical polymerization. Noteworthy, these nanoparticles were never tested before *in vivo*. Since too big nanoparticles cannot enter cells efficiently and too small particles cannot accumulate into tumors (after diffusion through the more permeable tumor endothelium), the control of the particle size was needed. This has been done by using the FDA approved surfactant, Lutrol F68. This original modification has led to nanoparticles with sizes of 60 nm instead of 200 nm as previously obtained without this surfactant. In fact, the isobutyl monomer is not soluble in water and will form a microemulsion during the energetic steering of the reaction medium. At low pH, anionic initiation of the polymerization is hindered. Only the cerium-induced radical on chitosan can initiate the polymerization leading to chitosan-coated nanoparticles. The use of the surfactant led to stabilize smaller size monomer droplets in the medium, resulting in smaller nanoparticles. Noteworthy, both poly(isobuthylcyanoacrylate) and chitosan were chosen because of their biocompatibility (37,38). The tolerance of the nanoparticles in mice can be confirmed since there was no reduction of the mice weight during the treatment. To our knowledge, the use

of these nanoparticles as vectors of biologically active macro-molecules was never done before. As they could ensure the presence of the siRNA in its intact form more than 2 days after intra-tumoral injection, these nanoparticles, associated with siRNA, were found to induce a significant inhibition of the tumor growth. Quantitative PCR of the ret/PTC1 oncogene shows a down-regulation of 82% of the ret/PTC1 oncogene in the tumor revealing that the siRNA is delivered in an active form inside the tumor. This result demonstrates the usefulness of these core-shell type nanoparticles for *in vivo* siRNA delivery. The mechanism needs to be explored. Indeed, the two most probable explanations for the efficiency of the method are either—an increase of the *in vivo* stability of the siRNA associated with nanoparticles, or retention of the siRNA inside the tumor. In this case, nanoparticles would play a role of a 'nanoimplant' inside the tumor. The *in vivo* efficiency comparison between free and vectorized stabilized siRNA (with O-methylation or LNA) could answer this question. Both protection of the siRNA and tumoral accumulation are the main goal for a vector development. The systemic injection has to be explored, as the intra-tumoral injection is only a preliminary investigative treatment. Because the enhanced permeability and retention effect can result in a passive tumor targeting, this treatment can be already used. Surface antibody grafting can be a nice improvement of the method, as this would allow having an active targeting.

Because of their dual composition, allowing to carry nucleotides at the surface and more hydrophobic compounds in the core, the nanoparticles described in this article could be further tested in association with other anticancer molecules.

ACKNOWLEDGEMENTS

We very much thank Dr Michel Kress (Andre Lwoff Institute, Villejuif) for the kind gift of the initial plasmid used for shRNA construction, Céline Ransy for Q-PCR helpful, Pr Martin Schlumberger for his interest in this work and Dr Dominique Costantini (Bioalliance Pharma) for her initial suggestions. We also acknowledge Jeril Degrouard for the TEM analysis and Bassim Al-Sakere (MD) for his help in animal experimentation and Andrei Maksimenko his help in technical support in fluorescence staining. The Budget Qualité Recherches of the Paris Sud University is gratefully acknowledged for the funding of this project. Henri de Martimprey was supported by a fellowship from the French Ministère de la Recherche et de la Technologie and the French Association pour la Recherche sur le cancer (ARC). We thank Florence Mc Bain for English corrections in this article. Funding to pay the Open Access publication charges for this article was provided by the CNRS.

Conflict of interest statement. None declared.

REFERENCES

1. Downward,J. (2004) RNA interference. *Brit. Med. J.*, **328**, 1245–1248.
2. Fuchs,U. and Borkhardt,A. (2006) The application of siRNA technology to cancer biology discovery. *Adv. Cancer Res.*, **96**, 75–102.
3. Raper,S.E., Chirmule,N., Lee,F.S., Wivel,N.A., Bagg,A., Gao,G.P., Wilson,J.M. and Batshaw,M.L. (2003) Fatal systemic inflammatory response syndrome in a ornithine transcarbamylase deficient patient following adenoviral gene transfer. *Mol. Genet. Metabol.*, **80**, 148–158.
4. Pouton,C.W. and Seymour,L.W. (1998) Key issues in non-viral gene delivery. *Adv. Drug Deliv. Rev.*, **34**, 3–19.
5. Jiang,H.L., Kim,Y.K., Arote,R., Nah,J.W., Cho,M.H., Choi,Y.J., Akaike,T. and Cho,C.S. (2007) Chitosan-graft-polyethylenimine as a gene carrier. *J. Control Release*, **117**, 273–280.
6. Je,J.Y., Cho,Y.S. and Kim,S.K. (2006) Characterization of (aminoethyl)chitin/DNA nanoparticle for gene delivery. *Biomacromolecules*, **7**, 3448–3451.
7. Gopal,V., Prasad,T.K., Rao,N.M., Takafuji,M., Rahman,M.M. and Ihara,H. (2006) Synthesis and in vitro evaluation of glutamide-containing cationic lipids for gene delivery. *Bioconjugate Chem.*, **17**, 1530–1536.
8. Takei,Y., Kadomatsu,K., Yuzawa,Y., Matsuo,S. and Muramatsu,T. (2004) A small interfering RNA targeting vascular endothelial growth factor as cancer therapeutics. *Cancer Res.*, **64**, 3365–3370.
9. MacLaughlin,F.C., Mumper,R.J., Wang,J., Tagliaferri,J.M., Gill,I., Hinchcliffe,M. and Rolland,A.P. (1998) Chitosan and depolymerized chitosan oligomers as condensing carriers for in vivo plasmid delivery. *J. Control Release*, **56**, 259–272.
10. Maksimenko,A., Polar,V., Villemeur,M., Elhamess,H., Couvreur,P., Bertrand,J.R., Aboubakar,M., Gottikh,M. and Malvy,C. (2005) *In vivo* potentialities of EWS-Fli-1 targeted antisense oligonucléotides-nanospheres complexes. *Ann. NY Acad. Sci.*, **1058**, 52–61.
11. Katas,H. and Alpar,H.O. (2006) Development and characterization of chitosan nanoparticles for siRNA delivery. *J. Control Release*, **115**, 216–225.
12. Howard,K.A., Rahbek,U.L., Liu,X., Damgaard,C.K., Glud,S.Z., Andersen,M.O., Hovgaard,M.B., Schmitz,A., Nyengaard,J.R. *et al.* (2006) RNA interference in vitro and in vivo using a chitosan/siRNA nanoparticle system. *Mol. Ther.*, **14**, 484.
13. Liu,X., Howard,K.A., Dong,M., Andersen,M.O., Rahbek,U.L., Johnsen,M.G., Hansen,O.C., Besenbacher,F. and Kjems,J. (2007) The influence of polymeric properties on chitosan/siRNA nanoparticle formulation and gene silencing. *Biomaterials*, **28**, 1208–1288.
14. Nikiforov,Y.E. (2002) RET/PTC rearrangement in thyroid tumors. *Endocr. Pathol.*, **13**, 3–16.
15. Di Cristofaro,J., Vasko,V., Savchenko,V., Cherenko,S., Larin,A., Ringel,M.D., Saji,M., Marcy,M., Henry,J.F. *et al.* (2005) ret/PTC1 and ret/PTC3 in thyroid tumors from Chernobyl liquidators: comparison with sporadic tumors from Ukrainian and French patients. *Endocrine-related Cancer*, **12**, 173–183.
16. Arighi,E., Borrello,M.G. and Sariola,H. (2005) RET tyrosine kinase signaling in development and cancer. *Cytokine Growth Factor Rev.*, **16**, 441–467.
17. Al-Brahim,N. and Asa,S.L. (2006) Papillary thyroid carcinoma: an overview. *Arch. Pathol. Lab. Med.*, **130**, 1057–1062.
18. Jhiang,S.M. (2000) The RET proto-oncogene in human cancers. *Oncogene*, **19**, 5590–5597.
19. Santoro,M., Melillo,R.M., Carlomagno,F., Fusco,A. and Vecchio,G. (2002) Molecular mechanisms of RET activation in human cancer. *Ann. NY Acad. Sci.*, **963**, 116–121.
20. Santoro,M., Melillo,R.M. and Fusco,A. (2006) RET/PTC activation in papillary thyroid carcinoma: European Journal of Endocrinology Prize Lecture. *Eur. J. Endocrinol./Eur. Fed. Endocr. Soc.*, **155**, 645–653.
21. DeLellis,R.A. (2006) Pathology and genetics of thyroid carcinoma. *J. Surg. Oncol.*, **94**, 662–669.
22. Mizuno,T., Iwamoto,K.S., Kyoizumi,S., Nagamura,H., Shinohara,T., Koyama,K., Seyama,T. and Hamatani,K. (2000) Preferential induction of RET/PTC1 rearrangement by X-ray irradiation. *Oncogene*, **19**, 438–443.
23. Nikiforova,M.N., Stringer,J.R., Blough,R., Medvedovic,M., Fagin,J.A. and Nikiforov,Y.E. (2000) Proximity of chromosomal

loci that participate in radiation-induced rearrangements in human cells. *Science*, **290**, 138–141.
24. Patel,K.N. and Singh,B. (2006) Genetic considerations in thyroid cancer. *Cancer Control*, **13**, 111–118.
25. Kim,D.H. and Rossi,J.J. (2007) Strategies for silencing human disease using RNA interference. *Nature Rev*., **8**, 173–184.
26. Scherr,M., Battmer,K., Schultheis,B., Ganser,A. and Eder,M. (2005) Stable RNA interference (RNAi) as an option for anti-bcr-abl therapy. *Gene Ther*., **12**, 12–21.
27. Toub,N., Malvy,C., Fattal,E. and Couvreur,P. (2006) Innovative nanotechnologies for the delivery of oligonucleotides and siRNA. *Biomed. Pharmacother*., **60**, 607–620.
28. Bertholon,I., Vauthier,C. and Labarre,D. (2006) Complement activation by core-shell poly(isobutylcyanoacrylate)-polysaccharide nanoparticles: influences of surface morphology, length, and type of polysaccharide. *Pharmaceutical Res*., **23**, 1313–1323.
29. Matsumura,Y. and Maeda,H. (1986) A new concept for macromolecular therapeutics in cancer chemotherapy: mechanism of tumoritropic accumulation of proteins and the antitumor agent smancs. *Cancer Res*., **46**, 6387–6392.
30. Fusco,A., Grieco,M., Santoro,M., Berlingieri,M.T., Pilotti,S., Pierotti,M.A., Della Porta,G. and Vecchio,G. (1987) A new oncogene in human thyroid papillary carcinomas and their lymph-nodal metastases. *Nature*, **328**, 170–172.
31. Barros,J.C. and Marshall,C.J. (2005) Activation of either ERK1/2 or ERK5 MAP kinase pathways can lead to disruption of the actin cytoskeleton. *J. Cell Sci*., **118**, 1663–1671.
32. Barone,M.V., Sepe,L., Melillo,R.M., Mineo,A., Santelli,G., Monaco,C., Castellone,M.D., Tramontano,D., Fusco,A. *et al*. (2001) RET/PTC1 oncogene signaling in PC Cl 3 thyroid cells requires the small GTP-binding protein Rho. *Oncogene*, **20**, 6973–6982.
33. De Falco,V., Castellone,M.D., De Vita,G., Cirafici,A.M., Hershman,J.M., Guerrero,C., Fusco,A., Melillo,R.M. and Santoro,M. (2007) RET/papillary thyroid carcinoma oncogenic signaling through the Rap1 small GTPase. *Cancer Res*., **67**, 381–390.
34. Bos,J.L. (2005) Linking Rap to cell adhesion. *Curr. Opin. Cell Biol*., **17**, 123–128.
35. Abbosh,P.H. and Nephew,K.P. (2005) Multiple signaling pathways converge on beta-catenin in thyroid cancer. *Thyroid*, **15**, 551–561.
36. Grimm,D., Streetz,K.L., Jopling,C.L., Storm,T.A., Pandey,K., Davis,C.R., Marion,P., Salazar,F. and Kay,M.A. (2006) Fatality in mice due to oversaturation of cellular microRNA/short hairpin RNA pathways. *Nature*, **441**, 537–541.
37. Quinn,J., Wells,G., Sutcliffe,T., Jarmuske,M., Maw,J., Stiell,I. and Johns,P. (1997) A randomized trial comparing octylcyanoacrylate tissue adhesive and sutures in the management of lacerations. *JAMA*, **277**, 1527–1530.
38. Mansouri,S., Lavigne,P., Corsi,K., Benderdour,M., Beaumont,E. and Fernandes,J.C. (2004) Chitosan-DNA nanoparticles as non-viral vectors in gene therapy: strategies to improve transfection efficacy. *Eur. J. Pharm. Biopharm*., **57**, 1–8.